AD-A143 790 DOPPLER SONAR AND PROFILING CTD OBSERVATIONS OF THE 1/1
INTERRELATIONSHIP BET..(U) SCRIPPS INSTITUTION OF
OCEANOGRAPHY LA JOLLA CA MARINE PHYSIC.. R PINKEL
UNCLASSIFIED 14 FEB 84 MPL-TM-359 N00014-79-C-0903 F/G 8/3 NL

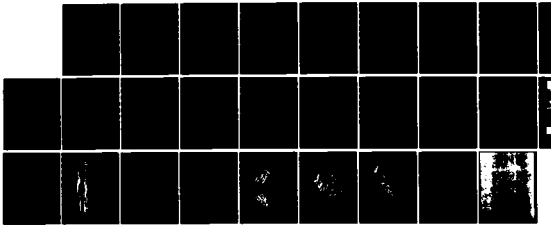

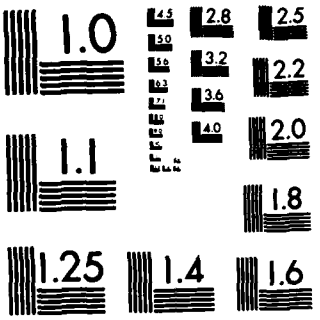

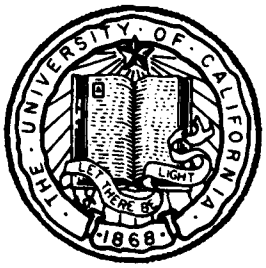

(1)

MPL TECHNICAL MEMORANDUM 359

AD-A143 798

Doppler Sonar and Profiling CTD Observations of the Interrelationship Between Large and Small Scale Internal Waves

by Robert Pinkel

Project Report for
Naval Ocean Research and Development Activity
Contract N00014-79-C-0983
Code 540

14 February 1984

MPL-U-29/83

MARINE PHYSICAL LABORATORY
of the Scripps Institution of Oceanography
San Diego, California 92152

Doppler Sonar and Profiling CTD Observations of the Interrelationship between Large and Small Scale Internal Waves

PROJECT REPORT

NORDA, Code 540

Rob Pinkel

University of California, San Diego
Marine Physical Laboratory of the
Scripps Institute of Oceanography
La Jolla, California 92093

Introduction

Over the past decade enormous progress has been made in the measurement of the various classes of motions in the sea. Specialized techniques have been developed to measure small scale turbulence, fine structure, internal waves, mesoscale eddies, and other phenomena. A current objective of considerable importance to both the Naval and the research communities is to understand the interrelationships and interaction between these various scales of motions. The ideal would be to be able to predict the occurance and evolution of small scale motions in the presence of the larger scale backgrounds.

At the Marine Physical Laboratory, two instrument systems have been developed for the purpose of bridging the gap between large and small scales. A profiling CTD was constructed in the early 1970's. This senses the vertical displacements in the sea by tracking the depths of isothermal or isopycnal surfaces. Vertical scales of

1 m to 400 m are resolved by the system. In the late 1970's Doppler sonar technology was developed. Sonars provide the capability to profile in directions other than vertical. Ranges in excess of 1 km can be sampled. However, the sonar range resolution is worse than the CTD, being approximately 20 m. The history of sonar development at MPL and a detailed description of the system are presented in Pinkel 1981a.

During May 1980 an upper ocean experiment was conducted using these systems on the Research Platform FLIP. Eighteen days of sonar and CTD data were collected as FLIP drifted slowly southward in the California current, approximately 400 km offshore. Support was obtained from Norda Code 540 to intercompare the data from these different sensing systems. Of particular interest is how these systems respond to the large scale shears in the upper ocean and how they measure the smaller scale wave motions which must propagate through these shears.

This report will document the view of the upper ocean as seen by the Doppler sonar and the CTD systems. Data from the May 1980 operation, as well as from earlier FLIP operations will be presented. Examples of depth-time series and power spectra will be presented for both systems. Combined wavenumber-frequency spectra will be used to demonstrate the relative amplitudes of the large scale-low frequency versus the small scale high frequency signals. Emphasis will be placed on the types of motions which are missed as well as measured by these two systems, as well as on disagreements in the measurements obtained.

Description of Experiment

On 25 April 1980 FLIP departed San Diego for a station at 31°N, 124°W, approximately 400 km offshore. From this position FLIP drifted slowly to the south for the next 30 days. The onboard instrumentation included a profiling array of current

meters developed by R. Weller of Woods Hole Oceanographic Institution (Weller, 1981). These profiled from 5 m to 150 m every hour. The profiling CTD (Pinkel, 1975; Occhiello and Pinkel, 1976) sampled between 4 and 400 m every two minutes. Approximately twelve thousand CTD profiles were collected during the trip. In addition four Doppler sonars mounted on FLIP's hull profiled 1100 m horizontally and 700 m vertically (Fig. 1). Two large (1.6 m diameter) sonars, operating at 80 and 85 kHz, were used in the horizontal measurements. These were mounted at a depth of 85 m, at right angles azimuthally. Two smaller (1.5 x 0.75 m) sonars were mounted at a depth of 38 m, angled 45^{o} downward, and operated at 70 and 75 kHz. This paper will discuss data from the downward slanting sonars only (Fig. 2).

Data collection began on 3 May, after several days of testing the sonar equipment. Operations ceased on 22 May when FLIP's H.P. 21 MX computer failed. Approximately 18 days of continuous data were colected, with a one-day gap on 12-13 May for data quality assessment. Prior to this gap 32 ms pings were transmitted every two seconds. The corresponding range resolution was 24 m. The associated depth resolution was 17 m for the slanting sonars. During the second, 11-day collection period, 40 ms pulses were transmitted every 1.5 seconds. These soner pulses improved the precision of the velocity estimates. The corresponding range and depth resolution is 30 and 21 m. The sonar echoes were complex demodulated, filtered with a 100 Hz lowpass filter and sampled at 300 Hz. The Complex Covariance technique of Rummler (1968) was used to estimate Doppler velocity. Velocity profiles were averaged over 5 minutes in time.

The time series measurements from each sonar can be easily interpreted only if the azimuthal orientation of the sonar remains relatively constant throughout the measurement period. An automatic orientation control system is used to regulate FLIP's heading. The system consists of a standard autopilot linked to the ship's

gyro compass. The autopilot controls a set of hydraulically operated propellers mounted approximately 5 m off FLIP's hull axis. Ths system was able to maintain heading at $320^{o} \pm 20^{o}$ true during the entire cruise. Typical heading stability was $+ 3^{o}$. Larger deviations resulted from passing squalls and frontal systems.

Velocity and Shear Spectra

The downward slanting Doppler sonars provide profiles of 45° slant velocity as a function of depth. (Fig. 3). These can be differentiated with respect to range to provide an estimate of the shear field. The differentiation cannot be done arbitrarily, however. The sonar profiles have finite range resolution (20 - 30 m for the May 1980 data). Taking the velocity difference with range over an interval shorter than this would tend to give an artificially small result. To investigate the effect of the differencing interval, several different intervals were tried. Power spectra of the shear calculated at two different intervals are presented in Fig. 4. The spectra are only moderately smoothed, hence they appear very irregular. Spectral slope varies between ω^{-2} and ω^{-1}. Note that as the differencing interval is increased the form of the shear spectrum approaches that of the classical ω^{-2} velocity spectrum. This is a consequence of the mathematics behind the analysis. If we consider two signals $u_1(t)$, $u_2(t)$ with power spectra $\langle u_1^2 \rangle (\omega)$, $\langle u_2^2 \rangle (\omega)$, the power spectrum of the <u>difference</u> between the two signals is just

$$\langle |(u_1 - u_2)|^2 \rangle (\omega) = \langle u_1^2 \rangle (\omega) + \langle u_2^2 \rangle (\omega)$$

$$-2\mathrm{Re} \langle u_1 u_2^* \rangle (\omega)$$

The difference spectrum is equal to the <u>sum</u> of the individual signal spectra minus twice the cospectrum, $C(\omega) = \mathrm{Re} \langle u_1 u_2^* \rangle$, between the signals. The magnitude of the cospectrum depends on the degree to which the two signals are coherent and are in phase. If the signals are perfectly coherent and in phase, the cospectrum between the two signals will equal the spectrum of either (identical) signal. If the coherent signals are 180° out of phase, the cospectrum will be the negative of the individual power spectra. If the signals are perfectly coherent but plus or

minus ninety degrees in phase, the cospectrum will vanish. Here the so-called quadrature spectrum

$$Q(\omega) = \mathrm{Im}\langle u_1 u_2^* \rangle (\omega)$$

will be large. The quadrature spectrum plays no role in the discussion of shear estimation, however. It is important to note that, as the two signals become less coherent, the magnitude of the cospectrum will be reduced. In the limit of zero coherence the spectrum of the difference between two signals is just the sum of the spectra of the individual signals.

With the sonar data, the relevant signals are the velocity time series at various ranges. If ranges too close together are used, the signals will be perfectly coherent, and the shear spectrum will be zero. The finite range resolution of the sonars tends to make nearby velocity series look identical. Thus, it is important not to use signals which are spatially separated by less than the resolution distance of the sonar. However, if series too far apart are used in the shear estimation, the signals will be incoherent. The resulting spectrum will be the sum of the individual velocity spectra. Nothing new will be learned about the ocean by taking their difference.

The shear spectra of Fig. 4 are typical of unsmoothed shear spectra obtained by other means. Two noteworthy aspects are that the dominant shear is at low frequency, and that the spectra are dominated by noise at frequencies above 2 cph.

It is difficult to assess the significance of the many irregularities in the shear spectra. It has been found useful to first difference these data in time prior to Fourier transformation to produce spectra which are 'white' in frequency. Significant irregularities are easier to detect against a flat spectral background.

Smoothed plots of the resulting acceleration (of velocity, not shear) spectra are presented in Fig. 5. These are formed by combining data from the two downward slanting sonars so as to obtain rotary spectra. The dark line corresponds to clockwise motion (viewed from above) while the lighter line to the counterclockwise motion. The spectra are plotted for two time periods during the May 1980 cruise. During the period 4-11 May both tidal and inertial signals were quite strong. These are seen in the left hand spectrum of Fig. 5. They dominate the low frequency portion of the clockwise spectrum. Higher frequency irregularities in the spectrum can be identified with harmonics of these low frequency peaks. The correspondence between spectral peaks and the theoretical position of harmonic lines is less than perfect. During the period 12-22 May 1980 the tidal and inertial signals are much weaker. Interestingly, the higher frequency bands of the spectrum are smaller also. Note the apparent harmonics of the inertial peak in the counter clockwise spectrum.

The drawback with the May 1980 Doppler data is that they are too noisy to resolve the highest frequency motions in the internal wavefield. The spectra sink into noise at about the frequency of the Vaisala cut off. Subsequent improvements to the sonar system have significantly reduced the noise levels. However there is little useful information on the high frequency waves in the May 1980 acoustic data. Fortunately, the CTD system employed during the cruise measured the wavefield from a different perspective. This system has the accuracy to observe high frequency waves. In subsequent sections, the CTD data will be described and the sonar and CTD views of the wavefield will be compared.

Repeated CTD Profiling

As an alternative to measuring the velocity field directly, measurements of the oceanic temperature or density field are often used to infer motions in the sea. Both large scale displacements and small scale distortions of the temperature or

density profiles are of interest. The CTD (conductivity, temperature, depth) instrument is typically used for these measurements. Special purpose CTD's have been constructed for use from FLIP to monitor the small scale motion field. These employ sensors which are more rugged and less expensive than a convential CTD (Occhiello Pinkel, 1976). The vertical resolution is approximately 1 m in temperature and conductivity, five meters in density. The sensors are cycled vertically through 400 m some 700 times a day in the course of a fine scale study of the upper ocean. During the May 1980 trip approximately 12,000 CTD profiles were obtained.

A representative sequence of profiles, obtained over a 24 hour period, is presented in Fig. 6. To avoid visual clutter, only every third profile obtained is plotted. These are separated by 6.6 minutes, rather than the originals 2.2 minute separation. The small scale features in the profiles are termed fine structure. They are, in part, the signature of the vertical straining of the sea by the internal wavefield. Fine structure also results from the horizontal advection or intrusion of water masses of differing temperature and salinity (but similar density) from one region to the next. The difficulty in interpreting temperature measurements is that there is no way to distinguish between the signatures of small scale vertical straining and large scale lateral advection. The former is of direct interest to the O.M.P., the latter is of less interest.

The profiles in Fig. 6 were selected from the larger May 1980 data set because of the diverse phenomena which are illustrated. Note that there are two mixed layers at the start of the observations. The first extends down to 40 m and is colder (and presumably less salty) than the underlying water. The second mixed layer extends to appoximately 90 m. The interface between the two varies in a most intriguing matter during the 24 hour observation period. In the thermocline, between 90 and 200 m there is a strong fine structure signal. During the first few

hours of observations, the water is isothermal (zero temperature gradient) over several depth intervals. At depths below 200 m the fine structure signal is much less apparent. This is not due to a reduction in the number of intrusion or the amount of wave straining. The reduction in the visible signal is a consequence of the fact that the mean gradient which is being distorted is much smaller at great depth.

Repeated profile information has become available only recently. Previously the time evolution of the temperature field was observed only from moored temperature sensors. These produced a far different view of the upper ocean temperature field. In Figure 7 the profile data of Fig. 6 have been used to synthesize a set of fixed depth temperature time series. These are the time histories of temperature as it would have been measured by a thermistor chain with sensors every 6 meters in the vertical.

The irregular temperature fluctuations in Fig. 7 result from the vertical advection of the temperature profile past the reference (sensor) depths. The fluctuations do not look sinusiodal even though the vertical displacement of the wavefield varies much more smoothly in space and time. The irregularity is due to small scale variations in the mean profile. These cause a varying temperature signal ΔT for a given vertical displacement ΔZ. The very fine structure which is the signal in Fig. 6 serves to 'contaminate' the internal wave signal in Fig. 7.

It's interesting to note several quasi-horizontal lines which persist in the Fig. 7 record. These are the signatures of the isothermal layers noted in Fig. 6. Although the layers are advected vertically by the wavefield, their temperature changes but slowly (presumably due to lateral advective effects). Close inspection of the horizontal lines shows that they are actually made up of a variety of short line segments. For example, as a layer is lifted vertically by the wavefield, a

sensor which was reading constant temperature within the layer will find itself outside the layer. Its output will begin to vary in response to wave motion. However a new sensor at the next depth up will now find itself in the zero gradient region. It will assume the constant output, at the same temperature reported by the previous sensor. Thus the constant temperature lines appear as signatures of zero temperature gradient regions. It is easy to see this sort of effect in Fig. 7 because the temperature time series were generated at depths which were closely spaced compared to the typical thickness of the isothermal layers. With very sparse vertical data, as is typically obtained by moored chains or discrete instruments, it is not always possible to unambiguously interpret the data.

A more effective way to use the repeated profile data of Fig. 6 is to follow the depth variations of selected isotherms. Such a plot is presented in Fig. 8. Here, a series of 120 isotherms, each separated by approximtely .1 ^{o}C, are tracked. The dark areas of Fig. 8, where many isotherms are congregated, are regions of high vertical temperature gradient. Where the isotherms are well separated in depth the temperature gradient is small. The isothermal regions in Figs. 6, 7, manifest themselves as the large gaps between isotherms in Fig. 8. Note the gradual transfer of isotherms from below to above the low gradient region centered at 300 m between hours 16 and 24. This indicates a slow temperature decrease of this layer. The water itself is presumably not being cooled. Water of a cooler temperature is being laterally advected under FLIP during this period. Another example of this phenomena is seen at 125 m depth between hours one and fifteen.

Away from these regions of intrusive activity the isotherms serve as excellent tracers of the vertical displacement of the internal wavefield. Both low (several cycles per day) and high (several cycles per hour) frequency motions are present. The lower frequency motions have the greatest displacements. The higher frequen-

cies, while smaller, stand out in Fig. 8 due to their remarkable persistance with depth. It has been found that while many internal wave modes might contribute to the low frequency wave field, the first-mode completely dominates the high frequency motions.

The propagation of internal waves is strongly influenced by the distribution of stability (the profile of Vaisala frequency) in the sea. At any given depth, propagating motions can only exist at frequencies below the local Vaisala frequency. Over the 400 m vertical extent of Fig. 8 the Vaisala profile varies from approximately 10 cph (at 100 m) down to 4 cph (at 400 m). The highest frequency waves should be constrained to the upper portions of Fig. 8. An example of this is the very high frequency wave packet which is centered at hour 2 between depths of 140 and 200 m. These die out at depths below 200 m, while the isolated lower frequency 'lump' which occurs at hour 3 penetrates right down to 400 m.

Many other illustrations of this effect can be seen in Fig. 8. The point to emphasize is that the CTD, in contrast with the Doppler sonar, has little difficulty seeing the highest frequency large scale-internal waves which can exist in the sea. It should be cautioned that very small scale motions (1-50 cm) might co-exist with these larger scale motions and still be beyond the CTD's view. However the low frequency view of the wavefield is contaminated by the effects of lateral intrusions. The sonar provides superior information here. It would seem reasonable to combine the two types of sensing systems to get the best possible view of the motions in the upper ocean.

Isotherm Vertical Velocity Spectra

One can process the time series of Fig. 8 in a manner analogous to the Doppler velocity time series to produce power spectra. It is convenient to plot spectra of

vertical velocity rather than vertical displacement. The vertical velocity spectra, like the slant acceleration spectra, are of nearly ω^0 form. Small irregularities in the form are thus easier to see. A representative example is given in Fig. 9. The spectrum is logarithmically averaged, with 18 degrees of freedom in the lowest frequency band, 200 degrees in the highest. It is seen that the spectral variance is confined between the local Vaisala and inertial frequencies. The spectrum is essentially flat between tidal frequency and 1 cph, with a series of irregular peaks that are of marginal statistical significance. Properly recolored, this spectrum would correspond to a displacement spectrum of ω^{-2} form between tidal frequency and 1 cph. Above 1 cph the spectrum rises to a pre-cutoff peak. This corresponds to the high-frequency waves visible in Fig. 8. With only a few crests per group in the time domain, $\Delta \omega / \omega$ is of order 1 in the frequency domain. It is thus not surprising to see that this high frequency peak at 3 cph is $\simeq$ 3 cph wide

It is worthwhile to compare velocity spectra over many depths, as in Fig. 10. Here nine spectra from depths 147-193 m are plotted. The scale is appropriate for the shallowest spectrum. Deeper spectra are offset by successive -5 dB increments. The regularity of the lowest three spectral peaks is striking. The first peak is the semidiurnal tide. The second peak is at the sum of tidal and inertial frequencies. The third peak is the first harmonic of the tide. Note that the power in the internal tide increases by a factor of 10 over the 46 m between the upper and lower measurements.

It is also important to emphasize that the lowest frequency peak in Fig. 10 is not the same low frequency peak which dominates the Doppler velocity spectra. The Doppler spectra are dominated by near inertial motions with a period of nearly 24 hr (at 30°N) while the CTD measurements are dominated by the 12.4 hour tide. Since most of the shear in the sea is at near inertial frequencies, the shear signal is

largely missed by the CTD measurements. The reason for this is not mysterious: the ratio of horizontal to vertical motion in the internal wavefield is a function of frequency. At near inertial frequencies the motion becomes almost purely horizontal. There is no vertical displacement signal for the CTD to detect. At frequencies approaching the Vaisala frequency the motion becomes almost purely vertical. This provides a strong signal for the CTD. Very accurate sonars should be able to detect this high frequency signal also. However, since the high frequency wave velocities are less than approximately 1 cm/sec, the present generation of sonars is unable to resolve them.

Wavenumber-Frequency Spectra of Slant Velocity and Shear

The real strength of repeated profiling data, whether it be doppler acoustic or CTD, is that the observed motions can be filtered/described in terms of their spatial as well as temporal frequencies. Variations of wave energy with frequency might well be different for short waves than for long waves. Changes in wave energy with changing wave length might be different for low frequency waves than for high. The combined wavenumber-frequency spectrum is the appropriate statistical descriptor of these effects. Two dimensional spectral estimates are obtained by Fourier transforming the profile data in both space and time. The squared Fourier coefficients, properly averaged and normalized, constitute the spectral estimate.

Slant wavenumber-frequency spectra for the 45^{o} slant component of velocity in the direction 55^{o} - 235^{o} are presented in Fig. 11. The May 1980 Doppler data were used to form these spectra. The left spectrum gives the distribution of wave energy with wavenumber and frequency for waves with energy propagating upward. The right spectrum describes describes the waves with downward propagating energy. The spectrum is estimated at frequencies from 3×10^{-2} cph, below the inertial frequency, to

1 cph. The wavenumber variations are measured from just below 1 cycle per slant kilometer (one cycle per 700 m vertical) to one cycle per 30 meters. The spectra peak at the near inertial frequency at low wavenumber. Peak values are approximately 10^7 $(cm/sec)^2$ / (cph·cpm). The point to emphasize with these spectra is that the noise level is approximately 10^3 $(cm/sec)^2$ / (cph·cpm). Not only is the large scale near inertial peak well measured but motions at small scale or high frequency, which are a factor of ten thousand times less energetic, also stand out above the noise. This illustrates the enormous capabilities of the acoustic approach for tracking the evolution of small scale less energetic features in the presence of an energetic large scale low frequency shear. Sadly, the highest frequency internal waves have energy levels even smaller than are visible with this system. Improvements made to the Doppler system since the May 1980 cruise will hopefully reduce the spectral noise levels further.

The two dimensional spectra are dominated by a series of ridges at the inertial and tidal frequencies and their harmonics. At low wavenumbers, they have approximately ω^{-1}, to ω^{-2} spectral forms. At low frequency, the wavenumber dependence is approximately k^{-1} out to 1 cycle per 100 m. Beyond that point the spectrum drops extremely rapidly. The slope approaches k^{-6} in the near inertial band! This high wavenumber cutoff in the spectrum is one of the most significant discovereis of the program to date.

The cutoff is better visualized when the spectra are heavily smoothed in frequency, so as to remove the effect of the harmonic ridges. A smoothed version of Fig. 11 is presented in Fig. 12. Here the near inertial cutoff at low frequency is seen to merge continuously with a higher frequency spectral shoulder. The high wavenumber cut off suggests that waves of vertical scale less than 60 m (slant scale less than 100 m) do not exist as either free or force motions in the sea. There are

a variety of possible explanations for this phenomena, none of which are certain. The cutoff is perhaps a key clue in the mystery of how small scale motions interact with large. A proper physical interpretation of this feature is vital.

From the wavenumber frequency spectrum of velocity, a wavenumber frequency spectrum of shear can be obtained. Such a spectrum is presented in Fig. 13. The shear spectrum has the same frequency dependence as the velocity spectrum. The wavenumber dependence, however, is boosted by a factor of approximately k^2 relative to the velocity spectrum. This has the effect of emphasizing the largest wavenumbers. At low frequency, up to 10^{-1} cph, the May 1980 shear spectrum is band limited in wavenumber. Shear variance is concentrated at slant wavelengths between 100 m and 1 km. At high frequencies the shorter scales progressively dominate the spectrum. This high wavenumber dominance at high frequency stands in direct contrast to the observation in Fig. 8 that the lowest mode (longest length scales) dominate the high frequency wavefield. The source of this high wavenumber shear variance is not currently understood. It is seen in measurements from conventional current meters as well as Doppler sonars. Traditionally it is ascribed to fine structure contamination in the velociy data. (Muller, Olbers Willebrand, 1978). Understanding this source of high wavenumber shear variance represents a major research goal.

The Isotherm Wavenumber Frequency Spectrum

To emphasize the discrepancy between the velocity and isotherm displcement series at high frequency, a wavenumber-frequency spectrum of isotherm vertical velocity is presented in Fig 14. January 1977 data is used to form this estimate. Here both upward and downward propagating motions are presented together, at positive and negative vertical wavenumbers. Zero vertical wavenumber corresponds to the average vertical velocity signal over the 342 m depth interval analyzed here. At all

frequencies the zero wavenumber band has the dominant energy. This is particularly true for frequencies below the 12.4 hour tide. The slow drift of the temperature sensors affects the readings at all depths similarly. Hence it makes a large contribution to the zero wavenumber low frequency signal. In spite of the sensor drift, the M2 tide can be seen at a variety of wavenumber bands. The most visible signal in Fig. 14 is the large peak at zero wavenumber which occurs at high frequency, just below the Vaisala cutoff. This peak corresponds to the high frequency low mode motions that are so apparent in Fig. 8. The disagreement between velocity and isotherm measurement of the high frequency wavefield is well summarized in the comparison of Fig. 11 and Fig. 14. In the slant velocity spectrum, the higher the frequency, the more gentle the wavenumber dependence. In the vertical velocity spectrum the spectral slope increases with increasing frequency.

Conclusions

Over the last decade considerable effort has been expended at MPL to develop the capability to measure small scale motions in the sea in the context of the larger scale background. Considerable progress has been made, as evidenced by the spectra of Figs. 11, 14. However, the technical difficulties have not been completely overcome. The physical processes remain imperfectly understood. The disagreement between vertical velocity measurements with CTD's and horizontal velocity measurements with conventional current meters or Doppler sonars is an example of the state of our present understanding. It is not clear whether this is a measurement problem (fine structure contamination) or a clue to the true physics of the upper ocean.

The CTD is an appealing instrument to use in these studies. It is no longer considered an exotic device and the interpretation of the measurements is straightforward (Figs. 6, 7, 8). The CTD clearly has the sensitivity to resolve high

frequency internal wave motions. Yet it cannot sense the low frequency shear field in which the higher frequency motions must propagate, as the low frequency shears are associated with almost no vertical displacement. This becomes an increasingly larger problem as one moves to more polar latitudes and the coriolis frequency decreases. At 75°N the vertical signature of the M2 tide disappears (F = 12.4 cph). Is one justified in extrapolating low latitude intuitions into polar regions in the absence of direct shear measurements? A related problem at high latitude is that the water is often isothermal to great depths, due to wintertime convection. The CTD provides no useful small scale information in such conditions.

Direct measurements of the velocity field are clearly preferred for use in regions where the water might be isothermal. Yet the existing generation of moored or profiling instruments is not adequate to resolve the smaller scale internal wave motions at high frequency.

Since the May 1980 cruise the MPL Doppler sonar system has been considerably improved. The velocity precision has been increased to the point where high frequency internal wave motions might be monitored. A major sea test, MILDEX, will be conducted in Fall 1983. At that time it is hoped that the discrepancy in the measurement of high frequency low mode internal will be resolved.

At this point the very issue is to understand how the small scale high frequency motions interact with the background shear. These small scale motions are currently measured only by special purpose microstructure devices. However, they are well within the measurement capabilities of so-called pulse to pulse coherent Doppler sonars. Such sonars have maximum range of a few tens of meters in contrast with the 1.5 km of the present incoherent sonars. However range resolution can be as small as a few centimeters. Measurements precise to 1 Hz in Doppler resolution can be obtained every few seconds! There has been no development history of these

devices in the Navy community, with the exception of a proof of concept demonstration done at MPL in the mid 1970's. This should be changed.

References

Muller, P., D. J. Olbers and J. Willebrand, 1978, The IWEX spectrum, J. Geophys. Res., 83, no. C1, 479-499.

Occhiello, L. M. and R. Pinkel, 1976, Temperature measurement array for internal wave observations, in Oceans '76, MTS, IEEE, 20E1-20E7.

Pinkel, R., 1975, Upper ocean internal wave observations from FLIP, J. Geophys. Res., 80, 3892-3910.

Pinkel, R., 1981a, On the use of Doppler sonar for internal wave measurements, Deep-Sea Res., 28A, no. 3, 269-289.

Pinkel, R., 1981b, Observations of the near-surface internal wavefield, J. Phys. Oceanog., 11, no. 9, 1248-1257.

Weller, R. A., 1981, Observations of the velocity response to wind forcing in the upper ocean, J. Geophys. Res., 86, no. C3, 1969-1977.

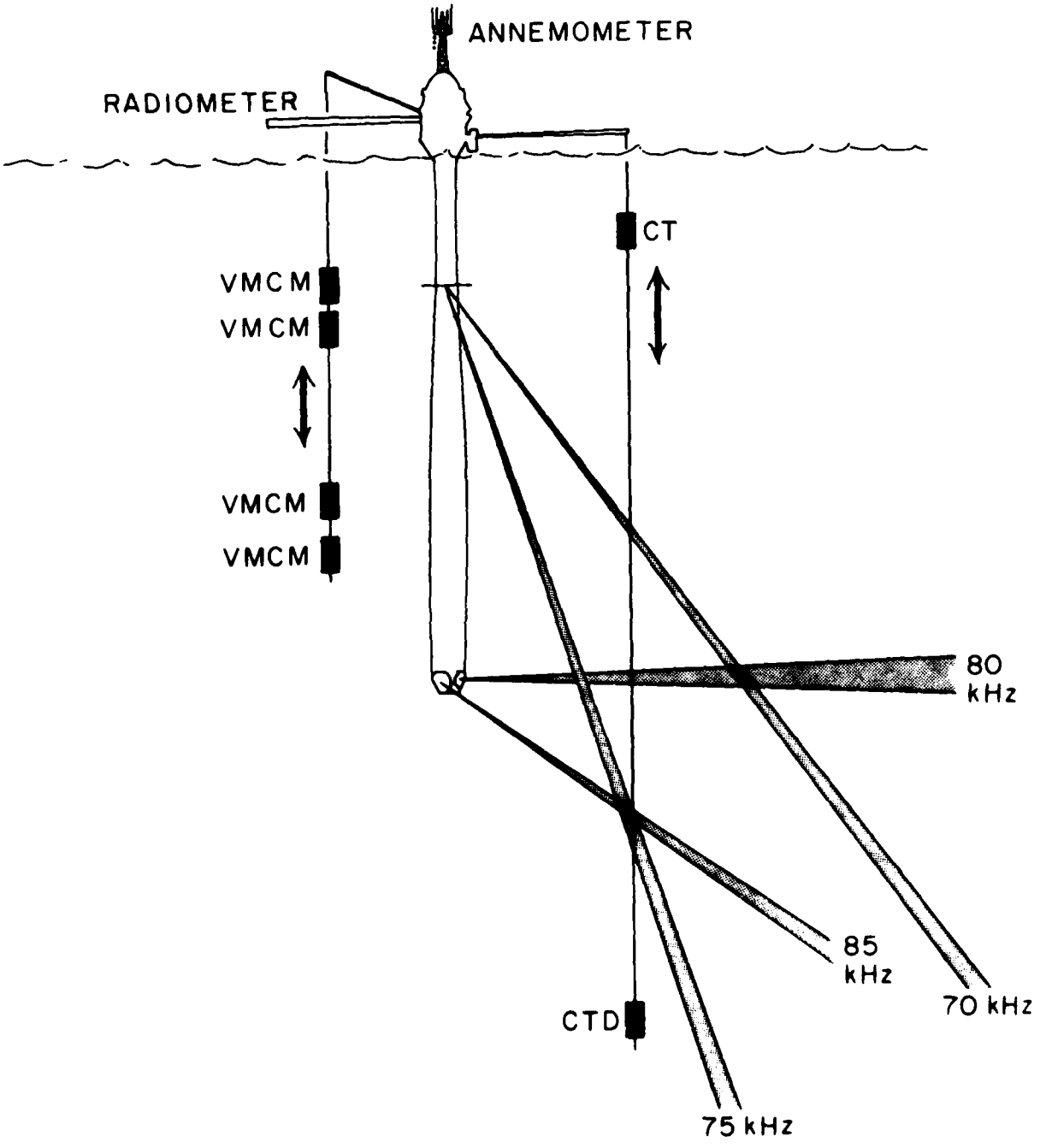

Fig. 1. Schematic of the May 1980 FLIP Experiment. The position of the four Doppler sonar beams is given by the grey areas. The VMCM current meters were generated by Dr. Robert Weller of Woods Hole.

Fig. 2. The 45° downward slanting Doppler sonars used to obtain the velocity and shear profiles. The sonars operate at frequencies of 70 and 75 kHz, at a peak power of 8 kW. The acoustic beam width is less than 1° in the vertical and approximately 2° in the horizontal.

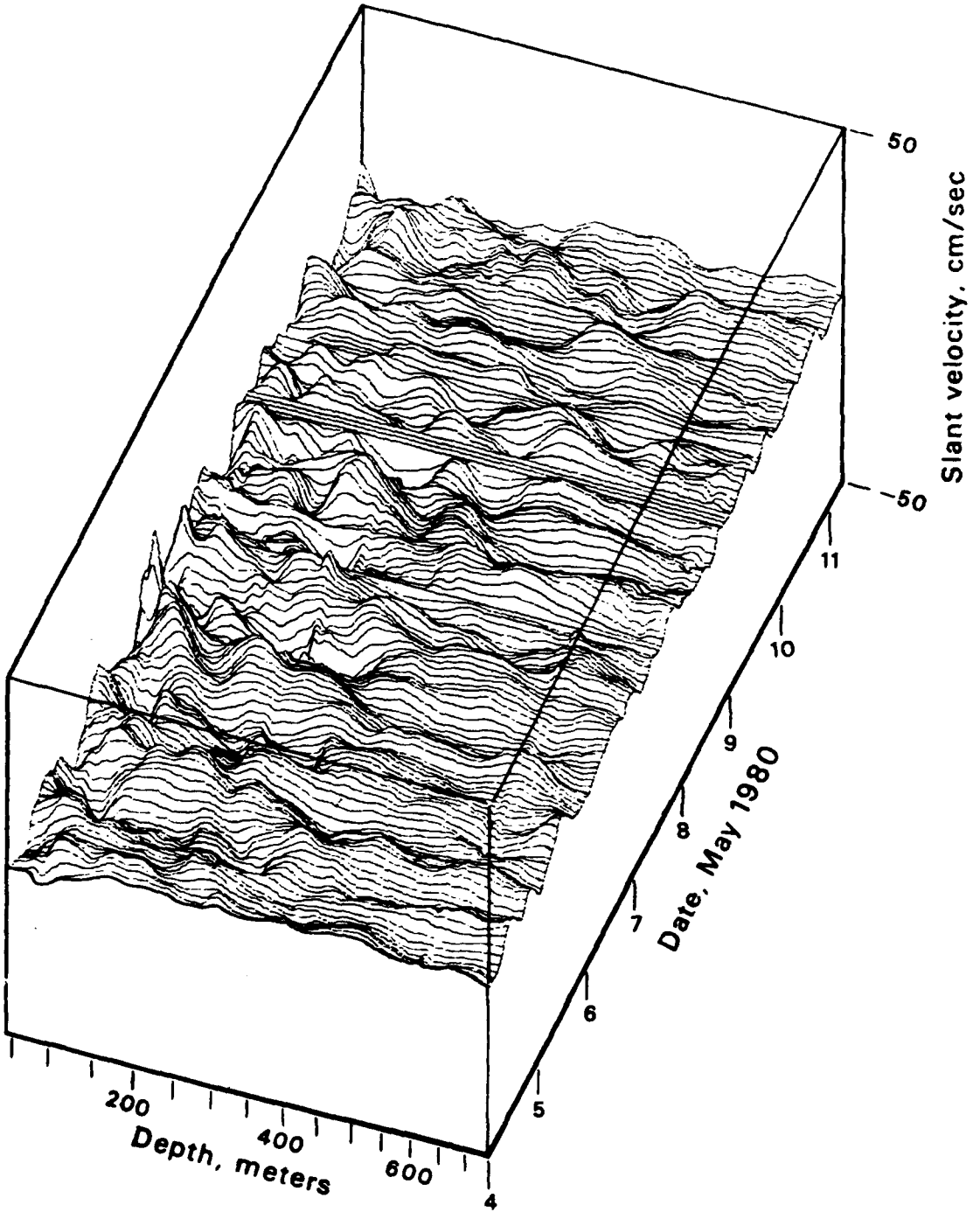

Fig. 3. Hourly profiles of velocity vs. depth and time obtained with the 70 kHz sonar. The first week of the May 1980 data set is presented.

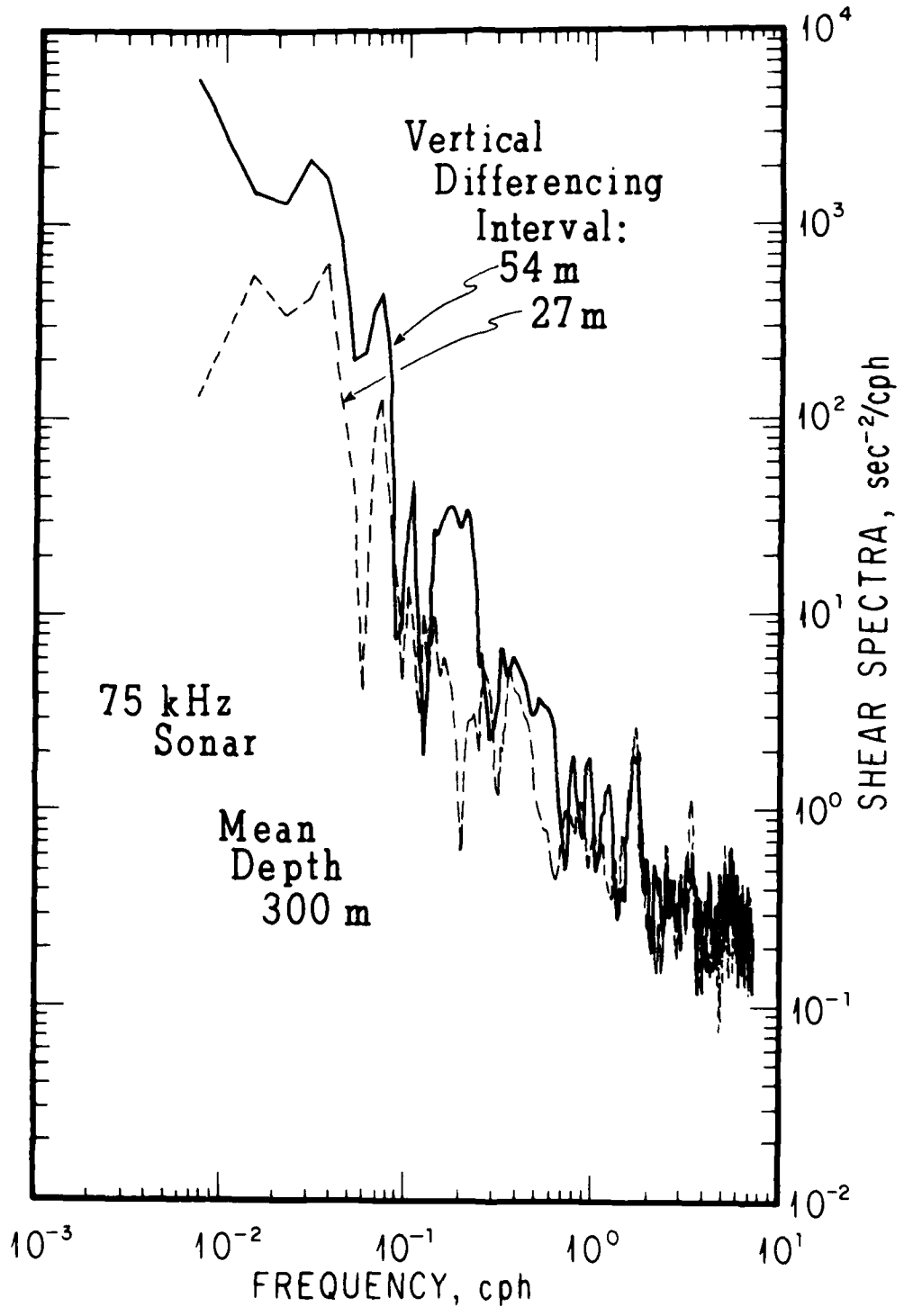

Fig. 4. Spectra of velocity shear obtained by differeing the Doppler velocity range-time series (Fig. 2) with respect to range. Spectra are presented for a depth centered at 300 m with differing intervals 27 m and 54 m. The low frequency form of the spectrum with 54 m separation is very nearly ω^{-2}. With the smaller separation the slope is more gradual. The spectra fall into the noise at approximately 2 cph.

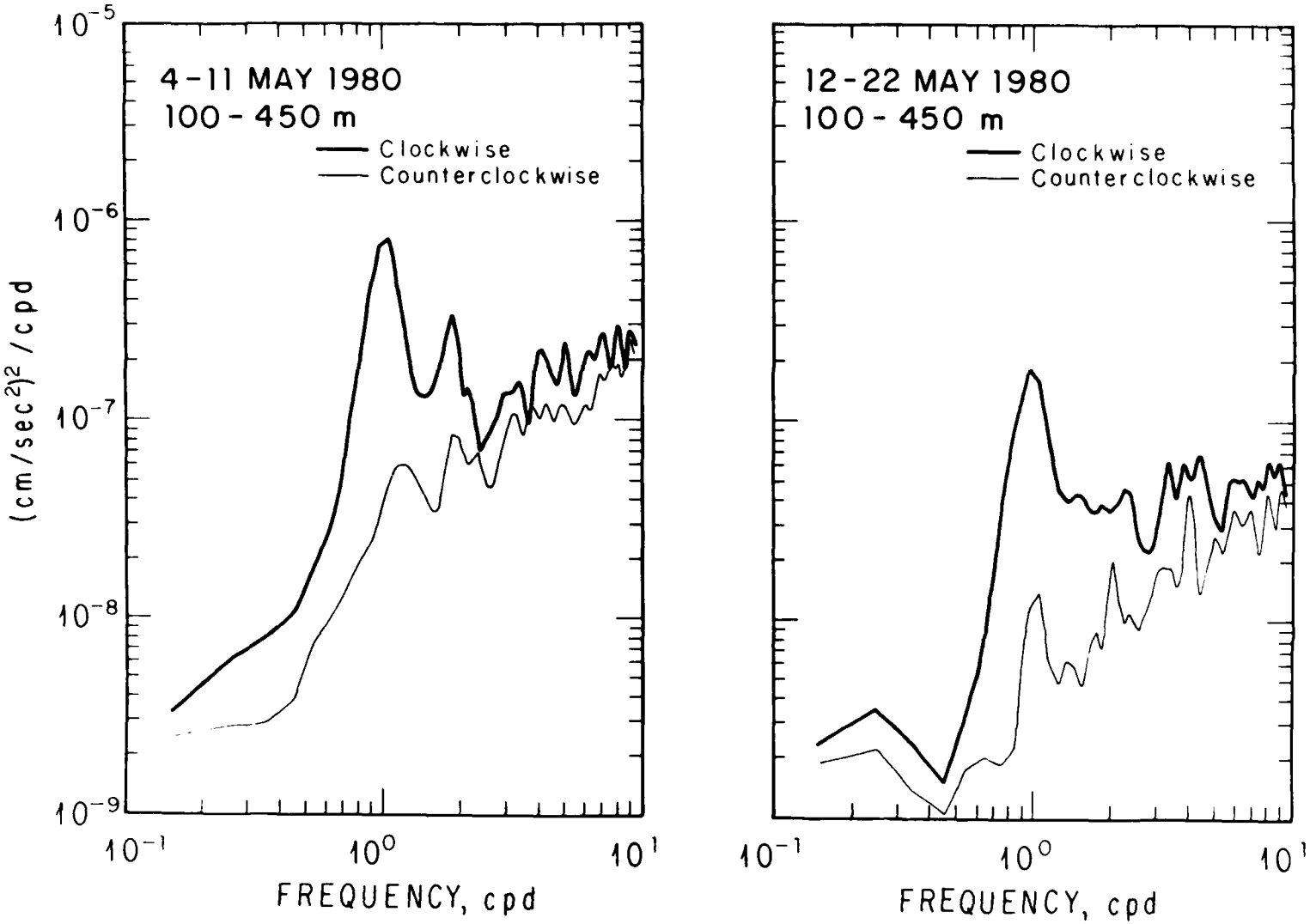

Fig. 5. Depth averaged rotary slant acceleration spectra, 3-11 May and 12-22 May 1980. Eight spectra, at 50 m intervals between 100 and 450 m, are combined to form each spectral estimate. There are nominally 64 degrees of freedom below 2.5 cpd, 192 degrees of freedom below 5 cpd. The actual statistical stability of this estimate is less than indicated by the number of degrees of freedom, as adjacent depths are not statistically independent. The clockwise spectra are indicated by the heavy lines.

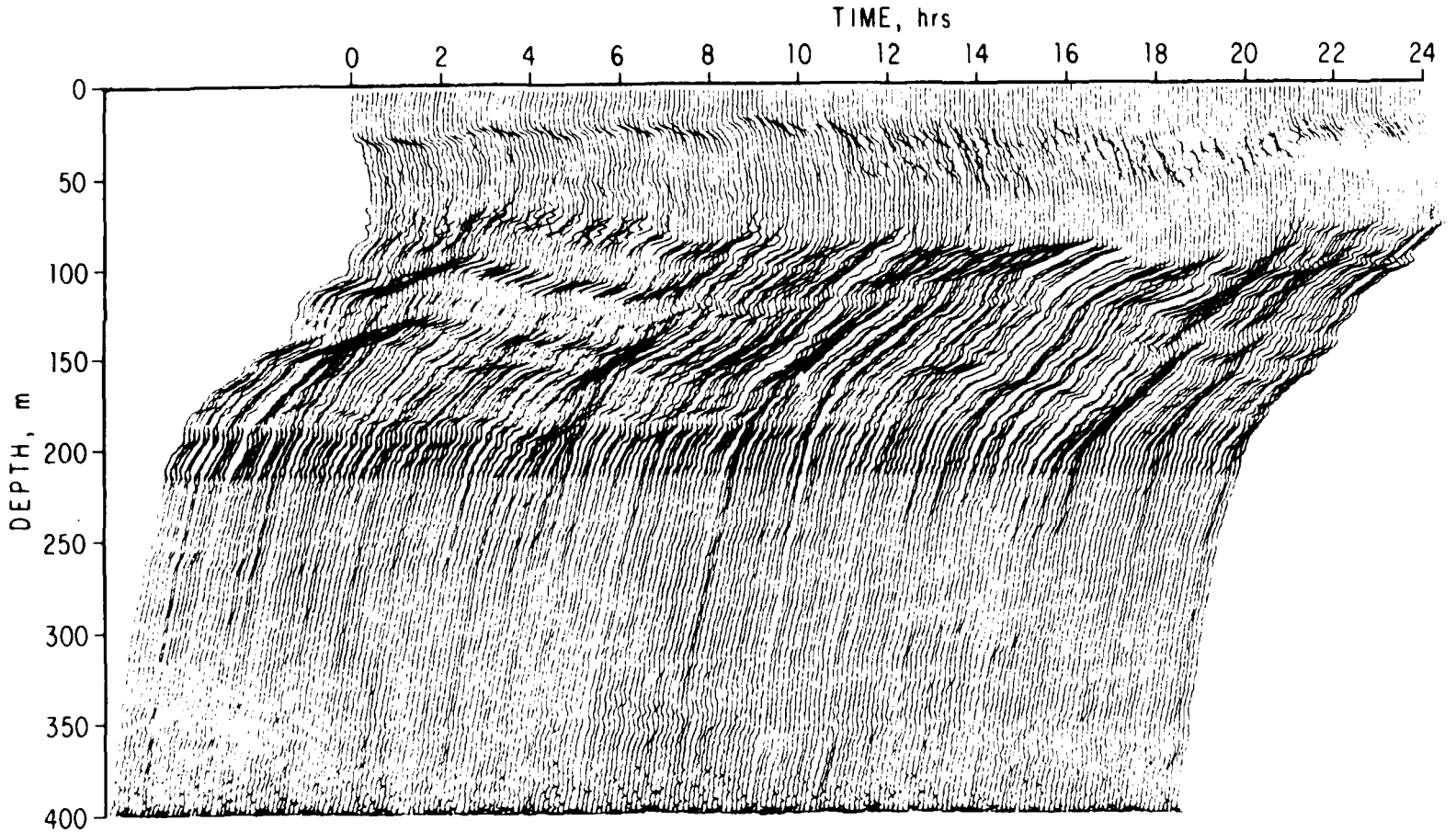

Fig. 6. A 24-hour sequence of temperature profiles obtained during the May 1980 FLIP cruise. Profiles are separated by approximately 6.6 minutes.

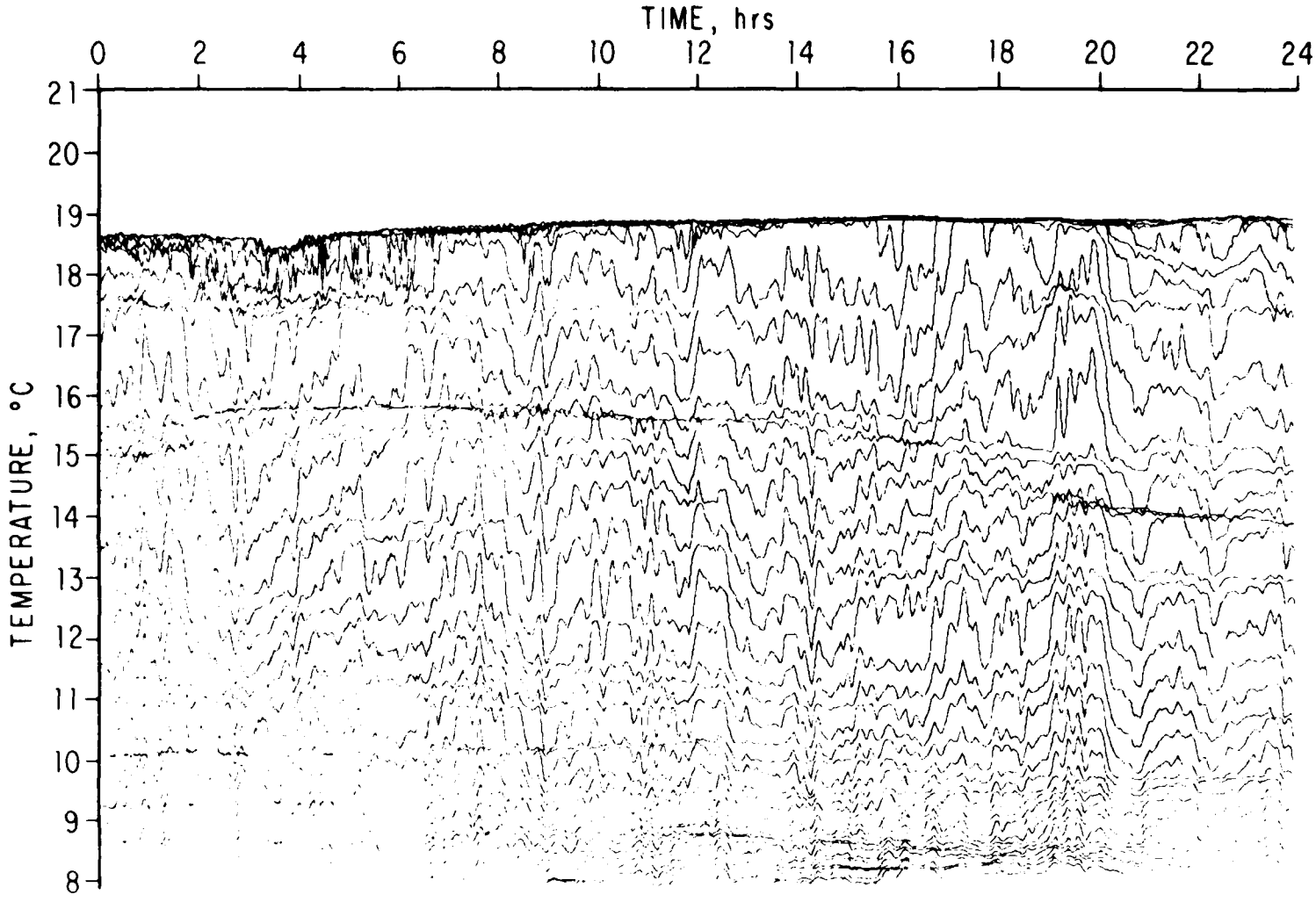

Fig. 7. Temperature fluctuations as a function of time at a series of fixed depths for the same time interval as in Fig. 6. The temperature fluctuations are tracked at a set of depths separated by 6 m over a depth range of 70 to 400 m. The quasi horizontal lines in these data correspond to nearly isothermal regions in Fig. 6.

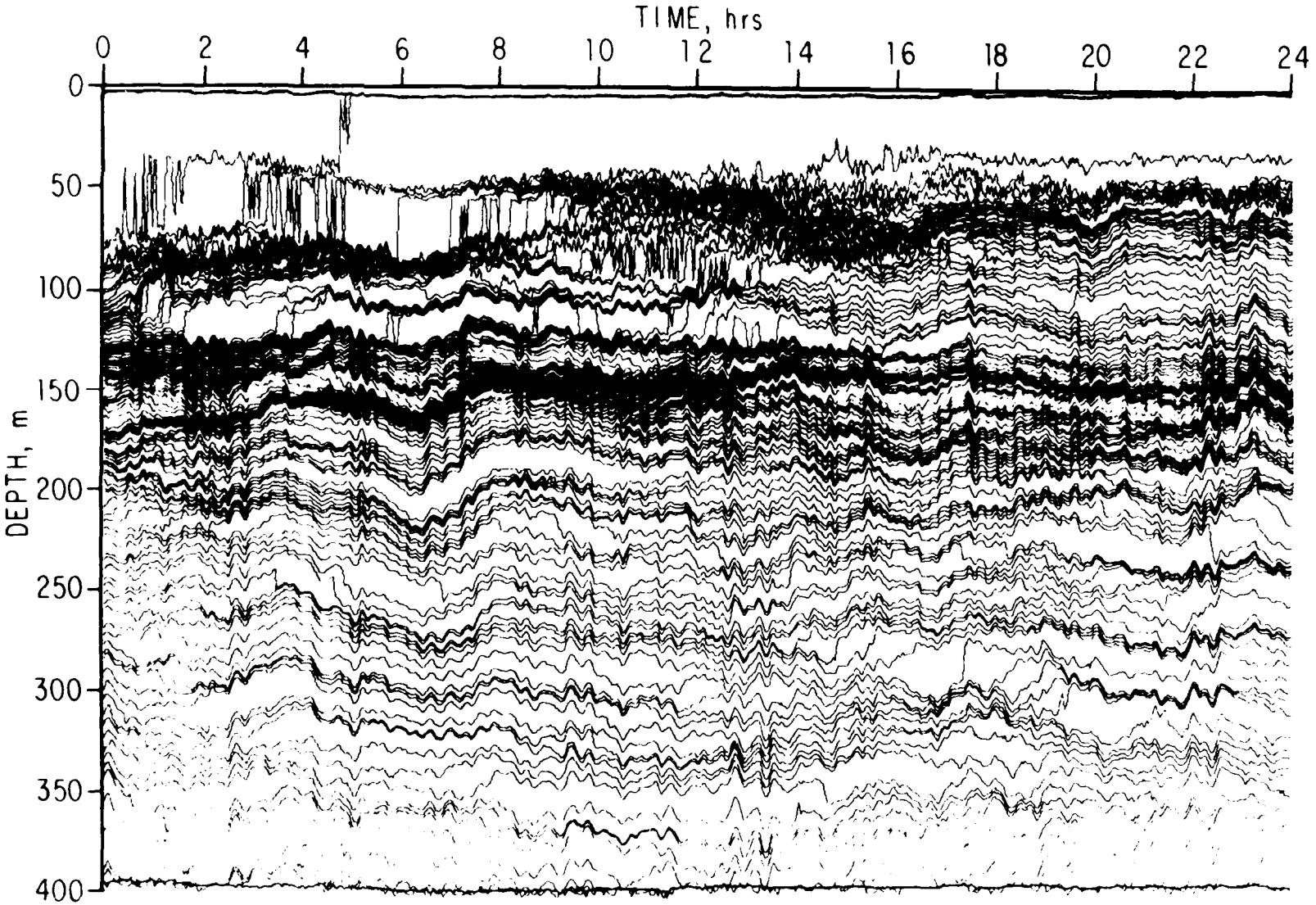

Fig. 8. Isotherm displacement time series for the same data interval as in Figs. 6, 7. The depths at which a set of 140 different temperatures occur are tracked from profile to profile to produce this view of the internal wavefield.

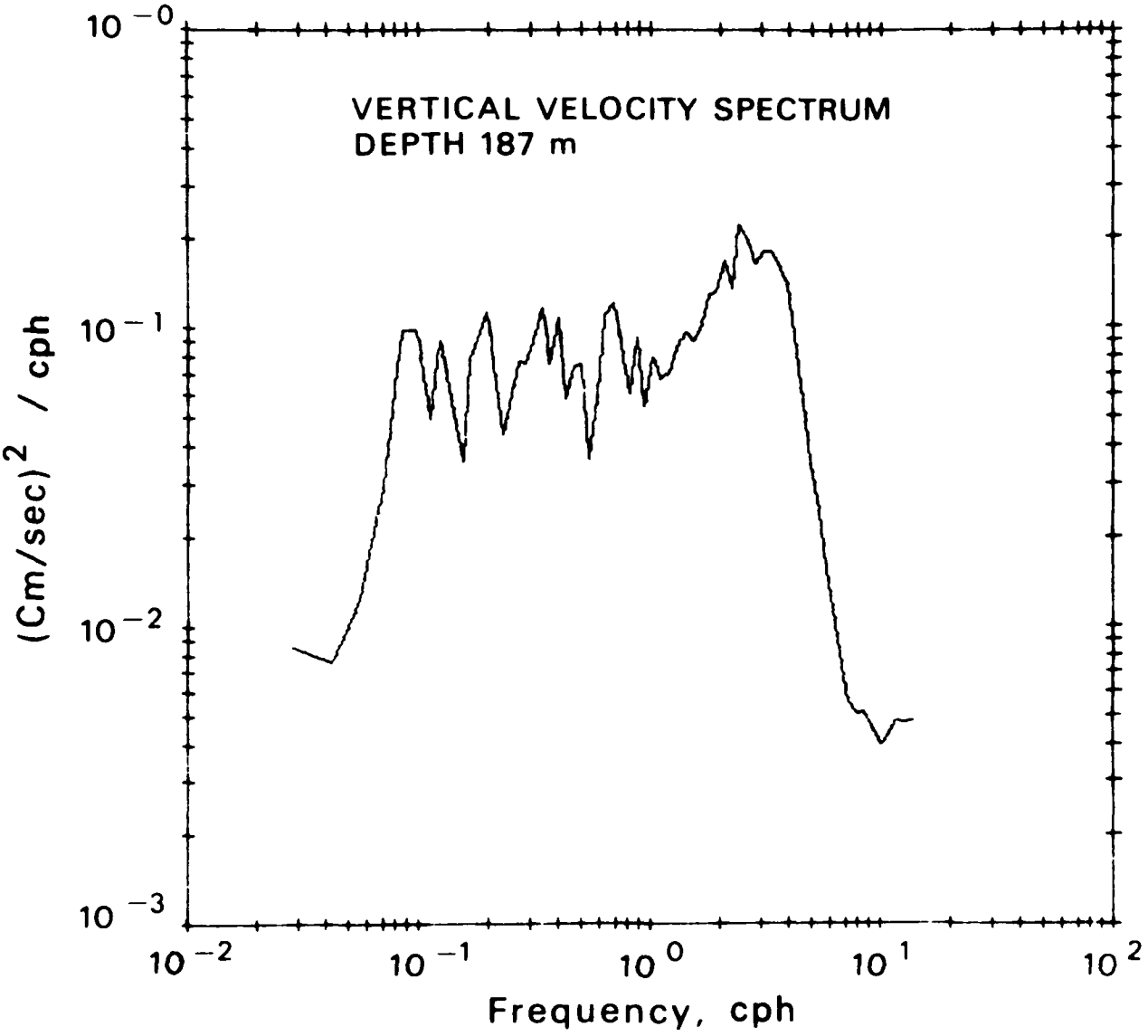

Fig. 9. A power spectrum of vertical velocity obtained from the profiling CTD. The spectrum is sharply confined between the inertial and Vaisala frequencies. The peak at the low frequency end of the spectrum is the 12.4 hr tide. The broad high frequency peak corresponds to low mock high frequency motions visible in Fig. 8.

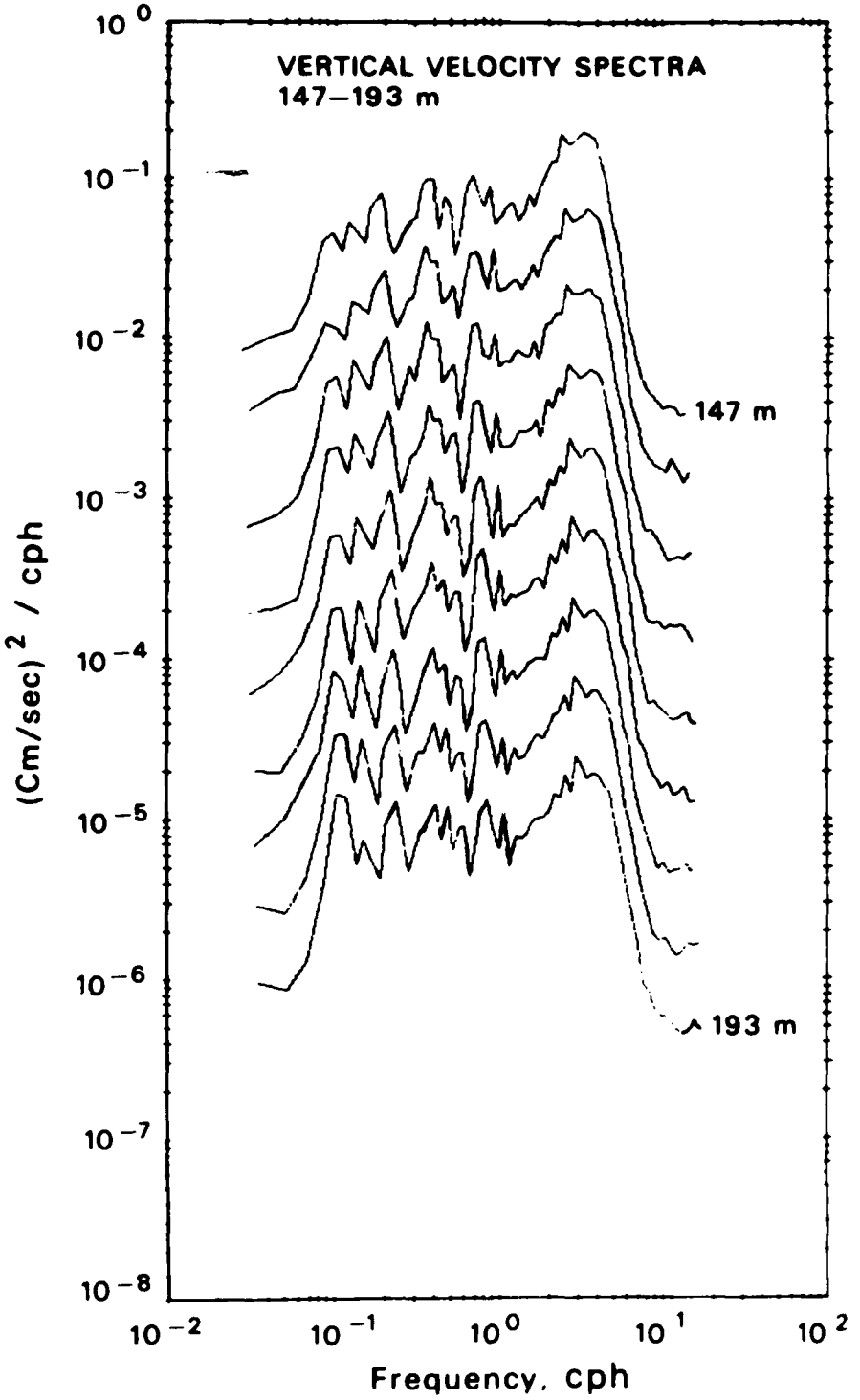

Fig. 10. A sequence of nine vertical velocity spectra over the region 147-193 m. The scale for the uppermost spectra is correct. Subsequent spectra are displaced by -5 dB. Solid arrows indicate the frequencies of the M2 tide and its first three harmonics. The dashed arrow marks the sum of inertial and tidal frequencies.

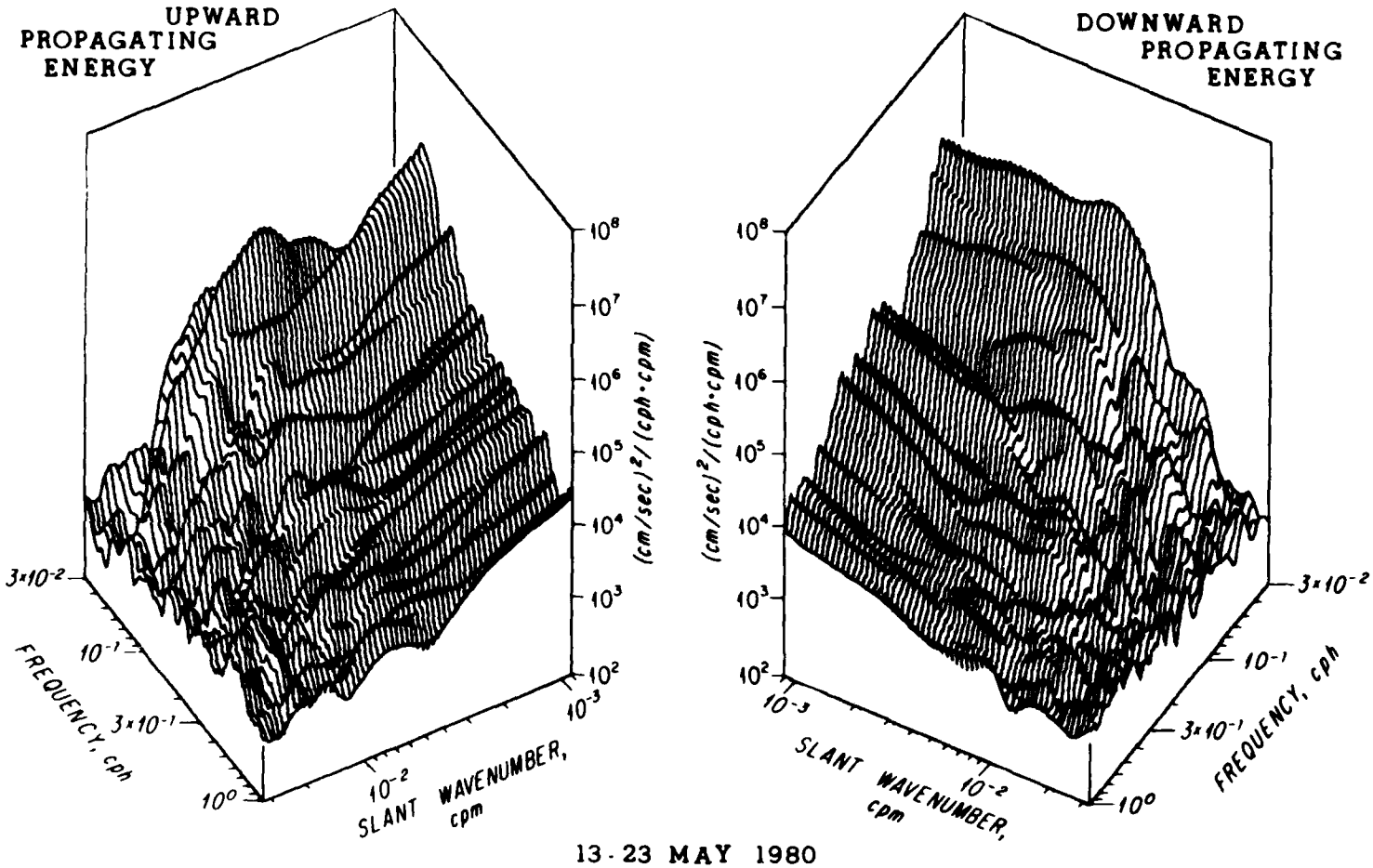

13-23 MAY 1980
29°-30° N, 124° W
VELOCITY IN DIRECTION 55° - 235°
70 kHz SONAR

Fig. 11. The wavenumber-frequency spectrum of the oceanic velocity field, as measured by the 70 kHz 45° downward slanting Doppler sonar. The low-frequency low wavenumber peak corresponds to near-inertial motions. The high-frequency high wavenumber motions are seen to have some ten thousand times less energy. It is necessary to further reduce the overall spectral noise level in order to get a clear view of this portion of the spectrum. Note the high wavenumber cut-off visible at low frequency.

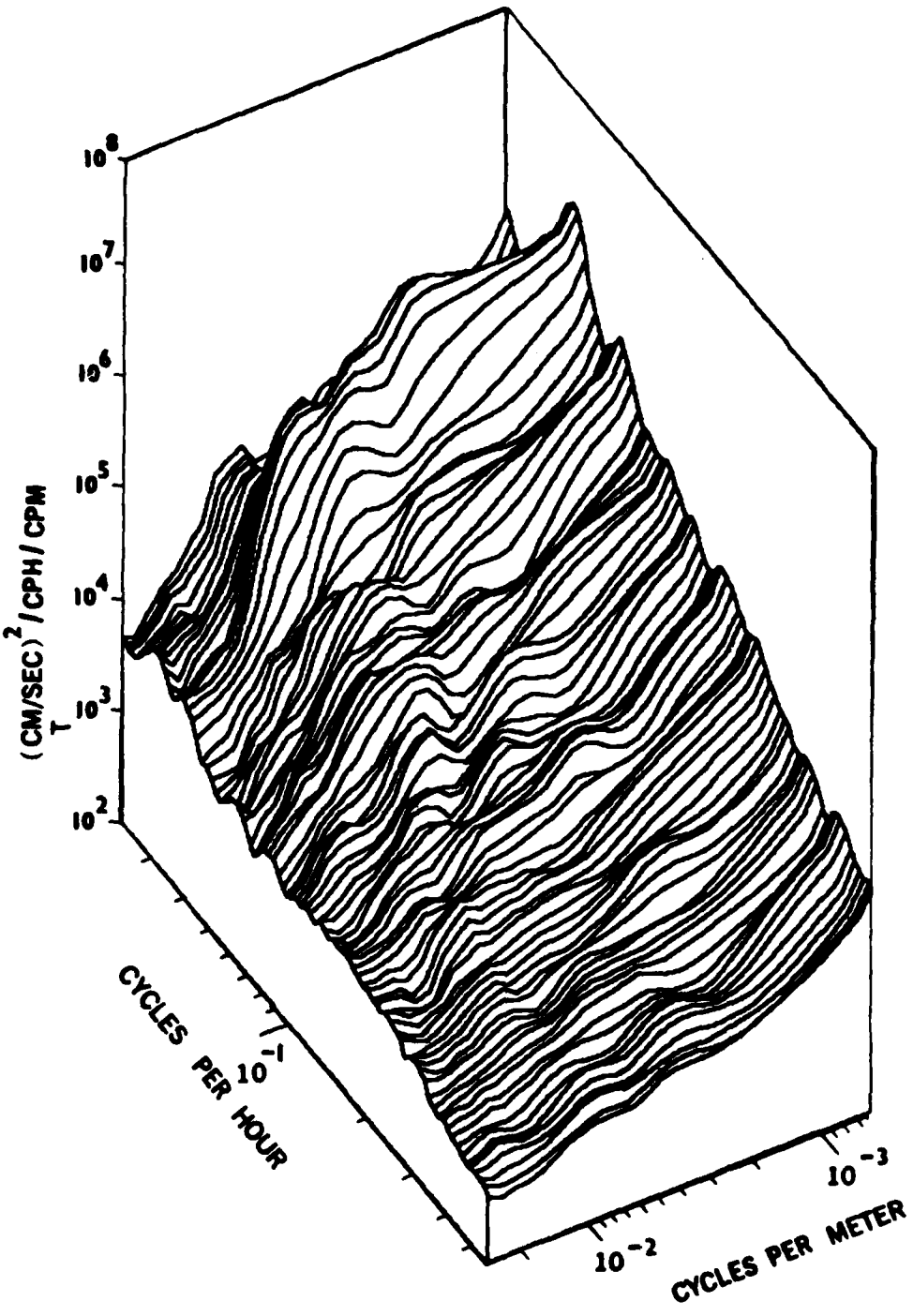

Fig. 12. A smoothed version of the spectrum presented in Fig. 11. When the ridges, which might correspond to harmonics of the tidal and inertial frequencies, are smoothed away, the low-frequency spectral shoulder and cut-off are seen to exentd to higher frequencies.

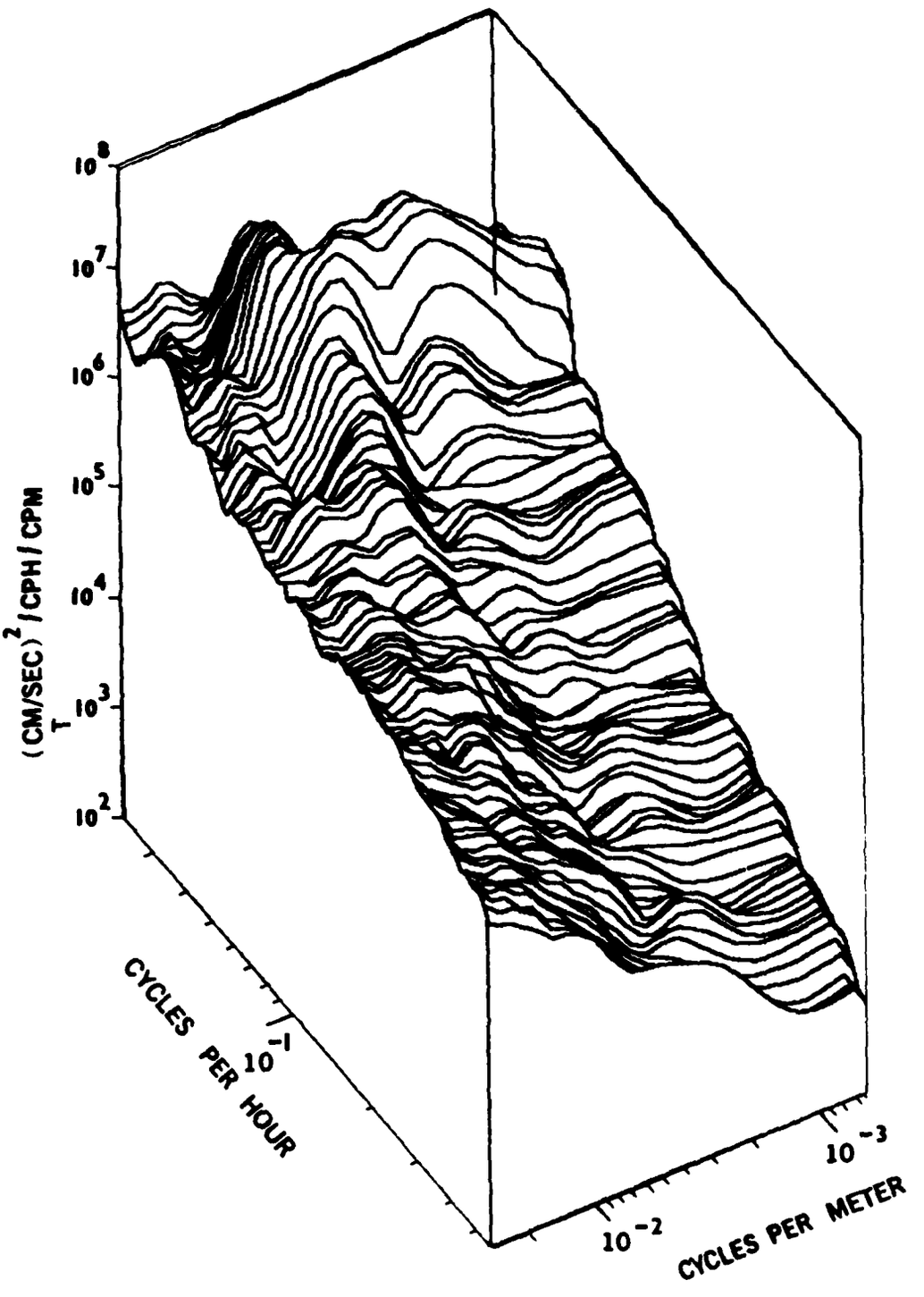

Fig. 13. A smoothed wave number frequency spectrum of the shear in the upper 700 m of the sea. This is obtained by differentiating the velocity profiles with respect to range, or alternatively weighting the 2-D velocity spectrum by a factor of k^0. The spectrum is band limited in wavenumber at low frequency, but becomes progressively more "blue" at higher frequency.

VERTICAL VELOCITY SPECTRUM AS A FUNCTION OF VERTICAL WAVENUMBER AND FREQUENCY

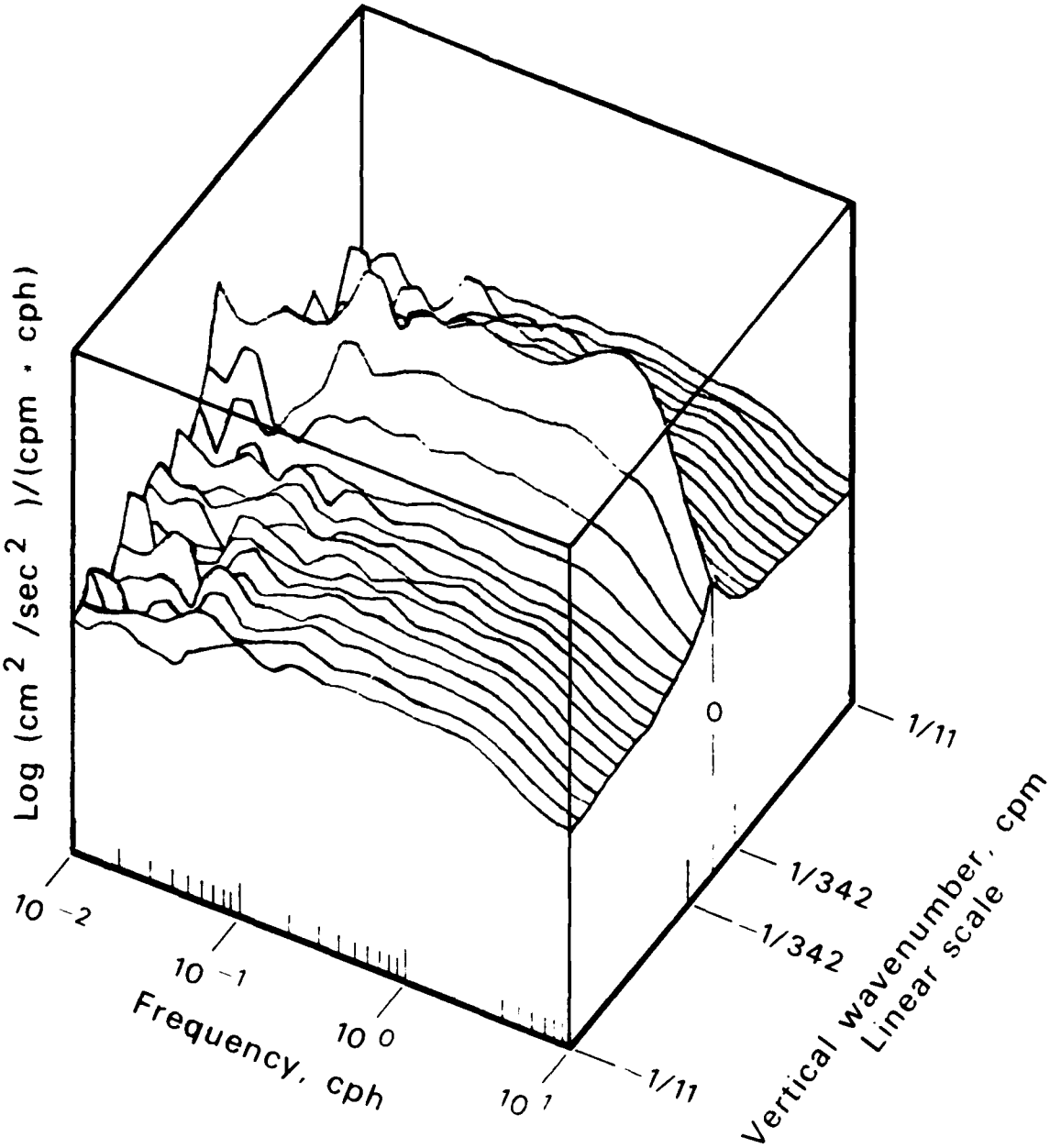

Fig. 14. A wavenumber-frequency spectrum of vertical velocity obtained with the profiling CTD. In contrast with the Doppler slant velocity spectrum, the vertical velocity spectrum is dominated by high-frequency motions. The spectrum is more strongly dominated by the longest vertical wavelengths at high frequency than at low. This disagrees with the picture obtained from the Doppler sonar (Fig. 11).

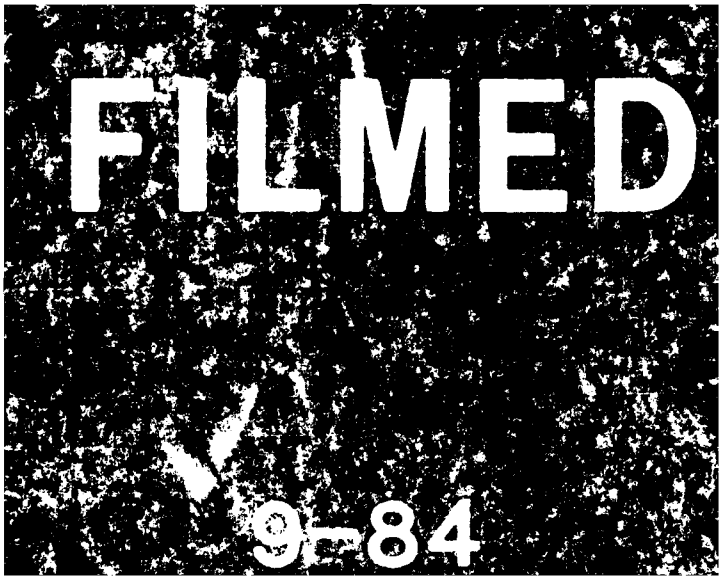
FILMED
9-84